23rd ABCM International Congress of Mechanical Engineering
December 6-11, 2015, Rio de Janeiro, RJ, Brazil

ASSESSING THE DYNAMIC PERFORMANCE OF KINEMATICALLY REDUNDANT MANIPULATORS

João Vitor de Carvalho Fontes
Maíra Martins da Silva
University of São Paulo - São Carlos School of Engineering , Department of Mechanical Engineering
joao.fontes@usp.br
mairams@sc.usp.br

Abstract. *Parallel manipulators have attracted the attention of academic and industrial communities due to their advantages over serial architectures. However, the singularities presented in the workspace of these manipulators cause some problems e. g. low precision and high torques. To avoid such problems, the kinematic redundancy can be applied to the architecture of the parallel manipulator. Considering these aspects, the objective of this paper is to measure the impact of the different levels of kinematic redundancy in the dynamic performance over the manipulators workspace. Four manipulators are evaluated, the non-redundant configuration 3RRR and three kinematically redundant configurations: the (P)RRR+2RRR, the 2(P)RRR+RRR and the 3(P)RRR. A dynamic index is proposed and calculated over the manipulators workspace. Such analysis allow the generation of dynamic maps which can be compared, highlighting the benefits on the dynamic performance by applying kinematic redundancy.*

Keywords: *parallel manipulators, kinematic redundancy, dynamic performance*

1. INTRODUCTION

For over a decade, parallel kinematic machines (PKM) have attracted the attention of academic and industrial communities due to their advantages over serial architectures. Among these advantages, it can be mentioned the lightness, the high speed/acceleration, the rigidity and the load capacity (Merlet, 1996). The most promising industrial application for these alternative architectures is the pick-and-place operation required in the food, pharmaceutical and electronic industries (da Silva *et al.*, 2010; da Silva and Gonçalves, 2013).

Although providing precision, high stiffness and good dynamic properties, the PKMs suffer from the presence of singularities in their workspace (Gosselin and Angeles, 1990; Bonev *et al.*, 2003). As a result, the ratio between the useful working space and physical space occupied by the equipment is rather low. Among other published works, Kotlarski *et al.* (2008); Mohamed and Gosselin (2005); Cha *et al.* (2007) have suggested that the use of kinematic redundancy can be a good alternative for minimizing the presence of singularities enhancing the workspace and can be capable of improving the dynamic performance and the precision of PKMs. Kinematic redundancy can be defined as the introduction of an active kinematic joint in a chain of a non-redundant mechanism as defined in Conkur and Buckingham (1997).

According to Mohamed and Gosselin (2005); Thanh *et al.* (2012), redundancy can increase the performance of PKM's and parallel machines can reconfigure itself according to different criteria and optimization strategies using an extra degree of freedom caused by the redundancy. The work of Cha *et al.* (2007) presents a manipulator with three levels of kinematic redundancy called 3R(P)RR. The inverse kinematic is proposed and an optimization is applied to avoid the singularities of the manipulator. The comparison between the redundant and non redundant manipulator showed that is possible to avoid the singularities and increase the workspace. Kotlarski *et al.* (2009, 2008, 2010, 2011) studied comparatively non redundant manipulators and manipulators with one level of kinematic redundancy. The aim of these works was to obtain a useful workspace with an acceptable precision and free of singularities. The results showed that the redundant manipulator is capable to reconfigure itself avoiding singularities and increasing the useful workspace. Fontes *et al.* (2014a,b); Ruiz *et al.* (2015) studied manipulators with different levels of kinematic redundancy and demonstrated that the redundancy can improve the dynamic performance and the energy efficiency of the PKMs.

Although the presented works showed an improvement of the characteristics of the manipulator when the kinematic redundancy is applied, the analysis of the presented works is highly dependent on the chosen trajectory. So, it is still an open question how much is the impact of the use of kinematic redundancy in the dynamic of manipulator considering the entire workspace of the manipulator. In order to infer about this quest, kinematic and dynamic models of the planar parallel manipulator 3RRR and the kinematically redundant planar parallel manipulators (P)RRR+2RRR, 2(P)RRR+RRR and 3(P)RRR., illustrated by Fig. 1, are exploited. As commonly used, the letter R corresponds to the revolute joint, the underline letter to the actuated joint and the number in front of the name refers to the number of kinematic chains. To explore the dynamic of the manipulator, a dynamic index is proposed and calculated over the workspace.

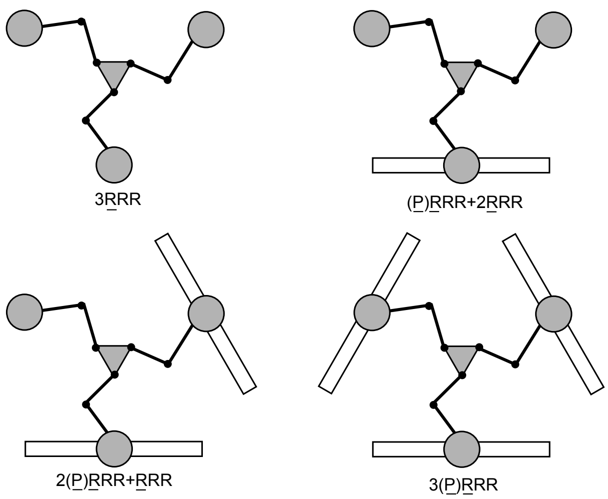

Figure 1. Non redundant manipulator and manipulators with kinematic redundancy

The numerical methodology employed to model the manipulators is briefly described in Section 2. The dynamic index also is detailed in the Section 2. The numerical results regarding this study are presented in Section 3. Finally, in Section 4, conclusions based on these numerical results are drawn.

2. NUMERICAL ANALYSES

The kinematic and dynamic model are presented in this section. The numerical analyses are treated briefly, but they can be found more detailed in Fontes *et al.* (2014a,b)

2.1 Inverse kinematic

The redundant manipulator is designed to form an equilateral triangle when $\delta_i = 0$, where δ_i is the position of the rotational motor relative of the center of each linear guide, in the way its barycenter is adopted as the origin of the base coordinate system, as illustrated in Fig. 2. The inverse kinematic is taken to determine the θ_i which is the rotation angle of the link A_iB_i, β_i, rotation angle of the link B_iC_i and, by optimization, δ_i explained in section 5. However, for the calculation of the kinematic inverse it is adopted an arbitrary δ_i.

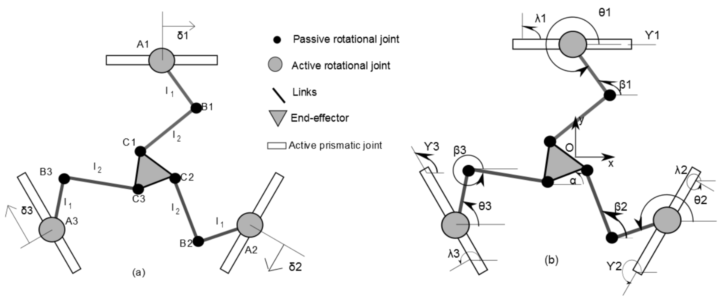

Figure 2. Kinematic model of 3(P)RRR: (a) Points and linear measures; (b) Angles and coordinate system

So, geometrically, the angles γ_i and λ_i are determined. Denote as a the length between the point O and the center of the linear guides, as h the length between the barycenter of the end-effector and any point C_i, l_1 and l_2 as the length of de link A_iB_i and B_iC_i, respectively.

Considering, the position vector of the point C_i can be written as:

$$r_{C_i} = r_{B_i} + l_2 \begin{bmatrix} cos(\beta_i) \\ sin(\beta_i) \end{bmatrix} \tag{1}$$

where r_{B_i} and r_{C_i} are the position vectors of the points B_i and C_i.

The angles θ_i and β_i can be calculated as:

$$\theta_i = 2\tan^{-1}\left(\frac{-e_{i1} \pm \sqrt{e_{i1}^2 + e_{i2}^2 - e_{i3}^2}}{e_{i3} - e_{i2}}\right) \tag{2}$$

$$\beta_i = \tan^{-1}\left(\frac{\rho_i - l_1\sin(\theta_i)}{\mu_i - l_1\cos(\theta_i)}\right) \tag{3}$$

where:

$$e_{i1} = -2l_1\rho_i \tag{4}$$

$$e_{i2} = -2l_1\mu_i \tag{5}$$

$$e_{i3} = \mu_i^2 + \rho_i^2 + l_1^2 - l_2^2 = 0 \tag{6}$$

$$\begin{bmatrix}\mu_i\\ \rho_i\end{bmatrix} = \begin{bmatrix}x\\ y\end{bmatrix} + h\begin{bmatrix}cos(\alpha+\lambda_i)\\ sin(\alpha+\lambda_i)\end{bmatrix} - \delta_i\begin{bmatrix}cos(\gamma_i)\\ sin(\gamma_i)\end{bmatrix} - a\begin{bmatrix}cos(\lambda_i)\\ sin(\lambda_i)\end{bmatrix} \tag{7}$$

2.2 Jacobian matrix

The jacobian matrix is defined as the matrix that relates the velocity vector of the actuators with the velocity vector of the end-effector. So, taken the time derivative of the Eq. (1), this relation can be determined:

$$\dot{x}[l_2\cos(\beta_i)] + \dot{y}[l_2\sin(\beta_i)] + \dot{\alpha}[l_2 h\sin(\beta_i - \lambda_i - \alpha)] = \dot{\theta}_i[l_1 l_2\sin(\beta_i - \theta_i)] + \dot{\delta}_i[l_2\cos(\beta_i - \gamma_i)] \tag{8}$$

where i is the kinematic chain adopted.

From the Equation (8), the matrix equation that relates $\dot{\Theta}$ and $\dot{X}$ can be expressed defining two matrices, A and B, with terms equal to:

$$a_{i1} = l_2\cos(\beta_i) \tag{9}$$

$$a_{i2} = l_2\sin(\beta_i) \tag{10}$$

$$a_{i3} = l_2 h\sin(\beta_i - \lambda_i - \alpha) \tag{11}$$

$$b_{ii} = l_1 l_2\sin(\beta_i - \theta_i) \tag{12}$$

$$b_{ii+3} = l_2\cos(\beta_i - \gamma_i) \tag{13}$$

where:

$$A = \begin{bmatrix}a_{11} & a_{12} & a_{13}\\ a_{21} & a_{22} & a_{23}\\ a_{31} & a_{32} & a_{33}\end{bmatrix} \tag{14}$$

$$B = \begin{bmatrix}b_{11} & 0 & 0 & b_{14} & 0 & 0\\ 0 & b_{22} & 0 & 0 & b_{25} & 0\\ 0 & 0 & b_{33} & 0 & 0 & b_{36}\end{bmatrix} \tag{15}$$

such that:

$$A\dot{X} = B\dot{\Theta} \tag{16}$$

The jacobian matrix can be expressed as:

$$J = A^{-1}B \tag{17}$$

2.3 Partial velocities and accelerations

The dynamic model is performed using virtual work. Thus, it is necessary to obtain matrices that relate the virtual displacements of each body of the manipulator with virtual displacement of the actuators. The relations between virtual displacements are equivalent to the relations between the velocities, so, as well the Jacobian matrix is for the end-effector, it must be obtained similar matrices for the other moving bodies of the system.

H_{ij} is defined as the matrix that relates the vector $\dot{\Theta}$ with the vector $\dot{r_{ij}}$ of linear velocity of the body j of the chain i. The rotational motor A_i receives value $j = 1$, the link A_iB_i receives $j = 2$ with pivotal point in A_i, and the link B_iC_i $j = 3$ with pivotal point in B_i. Similarly, the matrix G_{ij} relates the vector $\dot{\Theta}$ with angular velocity $\dot{\phi_i j}$. Consequently, H_{ij} and G_{ij} are sparse matrices.

Following this notation and all defined matrices can be generalized as:

$$K_{ij} = \begin{bmatrix} H_{ij} \\ G_{ij} \end{bmatrix} \tag{18}$$

So, the velocities can be calculated for each moving body of the manipulator:

$$\dot{d_{ij}} = K_{ij}\dot{\Theta} \tag{19}$$

where the vector d_{ij} is the combination of the linear and angular positions, $d_{ij} = \begin{bmatrix} r_{ij} \\ \phi_{ij} \end{bmatrix}$.

The accelerations are obtained by time derivative of velocities:

$$\ddot{d_{ij}} = K_{ij}\ddot{\Theta} + \dot{K_{ij}}\dot{\Theta} \tag{20}$$

2.4 Dynamic analysis

Once all the velocities and accelerations of each body were calculated, the Newton-Euler formulation is applied to each of the moving body about the corresponding pivotal point. In this analysis, it is assumed the mass of each motor in A_i, each link A_iB_i and each link B_iC_i is m_1, m_2 and m_3, respectively. The mass of the end-effector is m_n.

The vector p_{ij} is formed by the combination of forces and moments applied on the body j of the chain i:

$$p_{ij} = \begin{bmatrix} F_{ij} \\ M_{ij} \end{bmatrix} \tag{21}$$

Thus, all the information needed to apply the principle of virtual work are presented, so it is possible to determine the vector τ of required torques:

$$\tau = J^t p_n + \sum_{i=1}^{3}\sum_{j=1}^{3} K_{ij}^t p_{ij} \tag{22}$$

The vectors $\mathbf{p_{ij}}$ e $\mathbf{p_n}$ can be rewritten as:

$$\mathbf{p_{ij}} = Z_{ij} \begin{bmatrix} \ddot{r_{x_{ij}}} \\ \ddot{r_{y_{ij}}} \\ \ddot{\phi_{ij}} \end{bmatrix} + Nij \begin{bmatrix} \dot{r_{x_{ij}}} \\ \dot{r_{y_{ij}}} \\ \dot{\phi_{ij}} \end{bmatrix} \text{ , } \mathbf{p_n} = Z_n \begin{bmatrix} \ddot{x} \\ \ddot{y} \\ \ddot{\alpha} \end{bmatrix} \tag{23}$$

where:

$$Z_{ij} = \begin{bmatrix} m_j & 0 & -m_j s_{ij} \sin\phi_{ij} \\ 0 & m_j & m_j s_{ij} \cos\phi_{ij} \\ -m_j s_{ij} \sin\phi_{ij} & m_j s_{ij} \cos\phi_{ij} & I_j \end{bmatrix} \tag{24}$$

$$N_{ij} = \begin{bmatrix} 0 & 0 & -m_j \dot{\phi_{ij}} s_{ij} \cos\phi_{ij} \\ 0 & 0 & -m_j \dot{\phi_{ij}} s_{ij} \sin\phi_{ij} \\ 0 & 0 & 0 \end{bmatrix} \tag{25}$$

Performing the corrects transformations:

$$\boldsymbol{\tau} = M\ddot{\Theta} + V\dot{\Theta} \tag{26}$$

where:

$$M = (J^t Z_n J + \sum_{i=1}^{3}\sum_{j=1}^{3} K_{ij}^t Z_{ij} K_{ij}) \tag{27}$$

$$V = (J^t Z_n \dot{J} + \sum_{i=1}^{3}\sum_{j=1}^{3} K_{ij}^t Z_{ij} \dot{K_{ij}} + \sum_{i=1}^{3}\sum_{j=1}^{3} K_{ij}^t N_{ij} K_{ij}) \tag{28}$$

2.5 Dynamic index

In order to compare the manipulators, it is necessary to adopt a dynamic index that can be calculated across the workspace. Zhao and Gao (2009) propose a dynamic index consisting of fixing velocities and accelerations and calculate the torque required to perform these accelerations and speeds. Using this idea, the index proposed by this study is to evaluate how much torque is required to apply a module of acceleration 1 in all directions of the end-effector when it is at rest, that means $\dot{\mathbf{X}} = 0 \; and \; \dot{\mathbf{\Theta}} = 0$. The formulation of the index is shown below.

Considering the presented dynamic formulation and the velocities $\dot{\mathbf{\Theta}} = 0$, the Eq. (26) can be rewritten as:

$$M\ddot{\mathbf{\Theta}} = \boldsymbol{\tau} \tag{29}$$

Taking the time derivative of the Eq.(16), the accelerations of the active joints can be written as a function of the accelerations of the end-effector using the Jacobian matrix:

$$\ddot{\mathbf{\Theta}} = \dot{J^{-1}}\dot{\mathbf{X}} + J^{-1}\ddot{\mathbf{X}} \tag{30}$$

As the manipulator is at rest, $\dot{\mathbf{X}} = 0$ and using the definition of the Jacobian matrix, $J^{-1} = B^{-1}A$, the acceleration $\ddot{\mathbf{\Theta}}$ and the torques $\boldsymbol{\tau}$ can be calculated:

$$\ddot{\mathbf{\Theta}} = J\ddot{\mathbf{X}} \tag{31}$$

$$MB^{-1}A\ddot{\mathbf{X}} = \boldsymbol{\tau} \tag{32}$$

Considering all the accelerations $\ddot{\mathbf{X}}$ equal to 1:

$$MB^{-1}A\mathbf{1} = \boldsymbol{\tau} \tag{33}$$

where $\mathbf{1}$ is a column vector with elements equal to 1. The dynamic index DI is defined as the maximum required torque in the proposed conditions, which corresponds to the infinity norm of the matrix $MB^{-1}A$

$$DI = \left\| MB^{-1}A \right\|_{\infty} = max\left\{\boldsymbol{\tau}\right\} \tag{34}$$

The matrix B is not square so it was used the pseudoinverse of the matrix B. The index DI can be calculated all across the workspace because it is a function of the positions of the end-effector and the actuators. However the manipulators with kinematic redundancy have infinity possibilities of the position of the redundant joint, so it is necessary a search to find an optimum index to each position of the end-effector choosing a best position of the redundant joint.

In this way, it is possible to divide the linear guides in k points equally spaced and define which point is the best point of the linear guide to each point X of the mesh of the workspace that minimizes the index. It is necessary to highlight that singularities should be avoided, so the point of the linear guide must satisfy the condition ($\det A > 0$).

Tabela 1. Parâmetros utilizados para definir os manipuladores.

Parâmetro	Valor
m_1, m_n	$0.4kg$
m_2	$0.2kg$
m_3	$0.2kg$
l_1, l_2, a	$0.2m$
h	$0.05m$
δ_{max}	$0.3m$
I_1, I_2	$0.00667kgm^2$
I_n	$0.008kgm^2$

3. RESULTS

In order to compare the manipulators, the parameters are defined equally to all parameters. The parameters of the manipulators are presented in the Tab. 1.

Using dynamic content proposed in section 2.5, dynamic maps are designed for all manipulators. The index is calculated over the workspace considering the angular position of the end-effector equal to zero. These maps bring a better understanding of the dynamic study of manipulators. According to simulations of tasks was imposed a value limit of the dynamic index of 0.8. Therefore, if the index exceeds this value, the corresponding area is deemed to be unacceptable for execution of any task.

Figure 3a presents the dynamic map of the non-redundant manipulator 3RRR. It shows a red area that appears white. This area has singularities making very high torques in these areas in an attempt to perform any task, so this area is unacceptable. The other areas are covered with clear blue and green colors, which can be considered an average index.

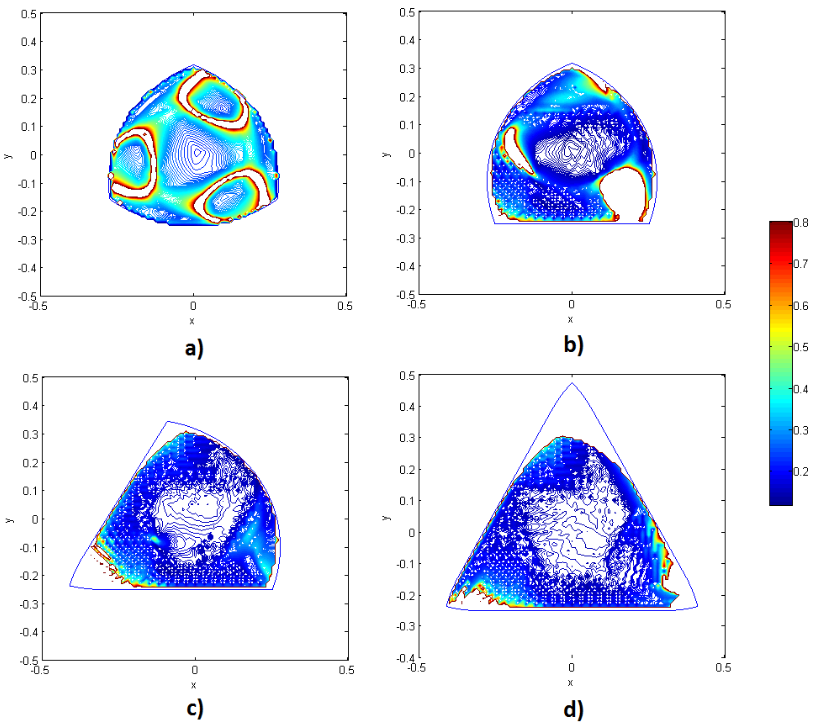

Figure 3. Dynamic maps of the manipulator: a) 3RRR; b) (P)RRR+2RRR; c) 2(P)RRR+RRR ; d) 3(P)RRR

Dynamic maps of the manipulators with kinematic redundancy are presented together with the workspace to show that even though the workspace increases with the addition of kinematic redundancy, it is not reachable for all angles of end-effector. As the angle is fixed at zero, some maps do not reach the limits of the workspace. The workspace is represented by a blue line that involves the dynamic maps.

The dynamic map of the manipulator (P)RRR+2RRR (Fig. 3b) has large dark blue area indicating a dynamic low rate, so this manipulator has high dynamic capabilities. However, it also has unacceptable areas because the manipulator has singularities as seen in the red and white areas.

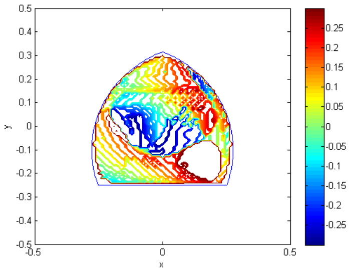

Figure 4. Optimal positions δ of the linear guides for each point of the workspace of the manipulator (P)RRR+2RRR.

Figure 4 shows the position of the linear guide needed to calculate the respective dynamic map. If one notes that in some areas the positions are homogeneous and can perform a smooth trajectory of the guide to reach all the optimal points along the workspace. However, to carry out an extensive trajectory of end-effector would be impossible to carry out a smooth trajectory to achieve the optimal points of the linear guide due to the break in continuity of the linear guide positions map.

The manipulator 2(P)RRR+RRR features a dynamic map (Fig. 3c) with a larger area in dark blue and does not have singularities, with a few limitations to reach the limit of the workspace due to the fixed angle the end-effector.

The manipulator 2(P)RRR+RRR also lacks the uniform optimal positions of the linear guides. As shown in Figure 5, it is impossible to achieve smooth trajectories to achieve the optimal points of the linear guides along the workspace due to non-uniformity of the maps of the optimal positions.

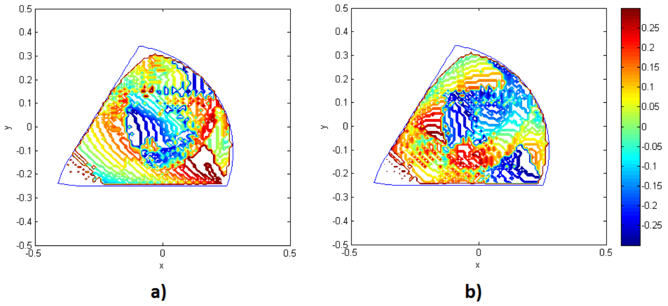

Figure 5. Optimal positions a) δ_1 b) δ_2 of the linear guides for each point of the workspace of the manipulator 2(P)RRR+RRR.

The dynamic map of the manipulator 3(P)RRR (Fig. 3d) has almost the same dark blue area that the dynamic map of the manipulator 2(P)RRR+RRR. Therefore, the addition of third level of kinematic redundancy does not bring any more dynamic benefit to the manipulator.

The optimal positions of the manipulator 3(P)RRR are depicted in Fig 6 and, like the other manipulators, are not uniform.

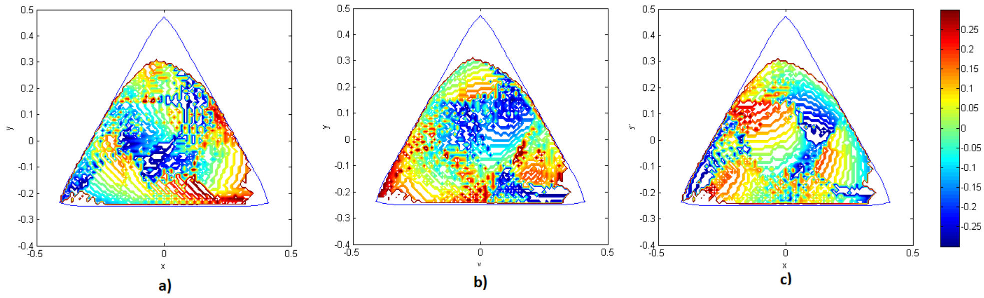

Figure 6. Optimal positions a) δ_1, b) δ_2 e c) δ_3 of the linear guides for each point of the workspace of the manipulator 3(P)RRR.

Comparing all dynamic maps, one can say that the the manipulator 2(P)RRR+RRR has a large work area with very good dynamic performance with fewer redundancy levels. The manipulator 3(P)RRR proved similar to the manipulator 2(P)RRR+RRR.

4. CONCLUSIONS

Based on the numerical results, one can conclude that kinematically redundant manipulators have greater dynamic capacities when compared to the non redundant manipulators. However, the kinematic redundancy is hard to be optimized for complex tasks because the impact on the improvement over the workspace is very oscillatory, that means the optimal position of the redundant joint is not smooth over the workspace. The authors suggest to implement some algorithm to penalize the break out of the optimal positions and calculate a feasible dynamic map.

5. ACKNOWLEDGEMENTS

The authors would like to thank CNPq and FAPESP (process n° 2014/01809-0) for the financial support granted.

6. REFERENCES

Bonev, I.A., Zlatanov, D. and Gosselin, C.M., 2003. "Singularity Analysis of 3-DOF Planar Parallel Mechanisms via Screw Theory". *Journal of Mechanical Design*, Vol. 125, No. 3, p. 573.

Cha, S.H., Lasky, T.A. and Velinsky, S.A., 2007. "Singularity Avoidance for the 3-RRR Mechanism Using Kinematic Redundancy". In *Proceedings 2007 IEEE International Conference on Robotics and Automation*. IEEE, pp. 1195–1200.

Conkur, E.S. and Buckingham, R., 1997. "Clarifying the definition of redundancy as used in robotics". *Robotica*, Vol. 15, No. 05, pp. 583–586.

da Silva, M.M., de Oliveira, L.P.R., Brüls, O., Michelin, M., Baradat, C., Tempier, O., Caigny, J.D., Swevers, J., Desmet, W. and Brussel, H.V., 2010. "Integrating structural and input design of a 2-DOF high-speed parallel manipulator: A flexible model-based approach". *Mechanism and Machine Theory*, Vol. 45, No. 11, pp. 1509–1519.

da Silva, M.M. and Gonçalves, L.A.M., 2013. "Mechatronic design concept and its application to pick-and-place robotic systems". *Journal of the Brazilian Society of Mechanical Sciences and Engineering*, Vol. 35, No. 1, pp. 31–40. doi:10.1007/s40430-013-0002-5.

Fontes, J.V.C., Santos, J.C. and da Silva, M.M., 2014a. "Torque optimization of parallel manipulators by the application of kinematic redundancy". *Conferência Nacional de Engenharia Mecânica - CONEM*.

Fontes, J.V.C., Santos, J.C. and Silva, M.M., 2014b. "Optimization strategies for actuators of kinematically redundant manipulators to achieve high dynamic performance". In *2014 Joint Conference on Robotics: SBR-LARS Robotics Symposium and Robocontrol*. IEEE, pp. 31–36.

Gosselin, C. and Angeles, J., 1990. "Singularity analysis of closed-loop kinematic chains". *IEEE Transactions on Robotics and Automation*, Vol. 6, No. 3, pp. 281–290. ISSN 1042296X.

Kotlarski, J., Abdellatif, H., Ortmaier, T. and Heimann, B., 2009. "Enlarging the useable workspace of planar parallel robots using mechanisms of variable geometry". In *Reconfigurable Mechanisms and Robots, 2009. ReMAR 2009. ASME/IFToMM International Conference on*. IEEE, pp. 63–72.

Kotlarski, J., Heimann, B. and Ortmaier, T., 2011. "Experimental validation of the influence of kinematic redundancy on the pose accuracy of parallel kinematic machines". In *Robotics and Automation (ICRA), 2011 IEEE International Conference on*. pp. 1923–1929.

Kotlarski, J., Thanh, T.D., Heimann, B. and Ortmaier, T., 2010. "Optimization strategies for additional actuators of kinematically redundant parallel kinematic machines". In *Robotics and Automation (ICRA), 2010 IEEE International Conference on*. pp. 656–661.

Kotlarski, J., Abdellatif, H. and Heimann, B., 2008. "Improving the pose accuracy of a planar 3(R)under-barRR parallel manipulator using kinematic redundancy and optimized switching patterns". In *2008 Ieee International Conference on Robotics and Automation, Vols 1-9*, IEEE, pp. 3863–3868.

Merlet, J.P., 1996. "Redundant parallel manipulators". *Laboratory Robotics and Automation*, Vol. 8, No. 1, pp. 17–24.

Mohamed, M.G. and Gosselin, C.M., 2005. "Design and analysis of kinematically redundant parallel manipulators with configurable platforms". *Robotics, IEEE Transactions on*, Vol. 21, No. 3, pp. 277–287.

Ruiz, A.G., Fontes, J.V.d.C. and da Silva, M.M., 2015. "The Impact of Kinematic and Actuation Redundancy on the Energy Efficiency of Planar Parallel Kinematic Machines". , No. 2009.

Thanh, T.D., Kotlarski, J., Heimann, B., Ortmaier, T., Do Thanh, T., Kotlarski, J., Heimann, B. and Ortmaier, T., 2012. "Dynamics identification of kinematically redundant parallel robots using the direct search method". *Mechanism and Machine Theory*, Vol. 52, No. 0, pp. 277–295.

Zhao, Y. and Gao, F., 2009. "Dynamic formulation and performance evaluation of the redundant parallel manipulator". *Robotics and Computer-Integrated Manufacturing*, Vol. 25, No. 4-5, pp. 770–781.

7. RESPONSIBILITY NOTICE

The authors are the only responsible for the printed material included in this paper.